

Novel Fiber-Reinforced Composites for Lightweight Ballistic Protection: A Structural and Performance Study



Rashid Faisal Mohammed^{*}, Waleed Bdaiwi[†]

Department of Physics, College of Education for Pure Science, University of Anbar, Anbar 31001, Iraq

Corresponding Author Email: ras22u3008@uoanbar.edu.iq

Copyright: ©2025 The authors. This article is published by IETA and is licensed under the CC BY 4.0 license (<http://creativecommons.org/licenses/by/4.0/>).

<https://doi.org/10.18280/rcma.350107>

ABSTRACT

Received: 14 January 2025

Revised: 10 February 2025

Accepted: 20 February 2025

Available online: 28 February 2025

Keywords:

ballistic resistance, composite materials, fiber-reinforced polymers, Kevlar-carbon-glass hybrids, adhesive formulations, impact and penetration testing

This study designs and evaluates two fiber-reinforced composite models for lightweight ballistic protection. Model One uses six layers each of Kevlar (KF), carbon (CF), and glass fibers (GF), with stainless steel mesh (CL) bonded by a hybrid adhesive of unsaturated polyester resin (UPS), natural rubber (NR), and corn starch (CS). Model Two features the same structure but with higher UPS content for improved bonding and stiffness. Mechanical properties, including impact resistance, hardness, tensile strength, compressive strength, and bending behavior, were systematically evaluated for both models. Field ballistic testing using 7.62×39 mm ammunition fired from a Kalashnikov (AK-47) rifle demonstrated both models successfully confined the projectile within the composite layers without complete penetration. X-ray imaging confirmed the structural integrity of the composites, as bullets remained embedded within the layers. Model Two exhibited superior structural impact resistance (150 kJ/m^2), compressive strength (222.07 MPa), and tensile stiffness (Young's modulus: 7.37 MPa), outperforming Model One, which showed higher ductility and energy absorption capacity (fracture strain: 33.3%). The results underscore the complementary strengths of the two models, suggesting their potential for hybrid designs. This study highlights the potential of fiber-reinforced composites in developing cost-effective, lightweight ballistic protection systems for personal and vehicular applications.

1. INTRODUCTION

Ballistic protection systems are essential for safeguarding individuals and structures against high-velocity projectiles. Traditional materials such as Kevlar, ultra-high-molecular-weight polyethylene (UHMWPE), and ceramics have long been the benchmarks for body and vehicular armor, offering high strength-to-weight ratios and exceptional impact resistance [1-3]. However, the use of these materials introduces trade-offs between weight, cost, flexibility, and multi hit performance, motivating the development of innovative composite solutions [4]. The integration of structural strength, energy absorption, and cost efficiency in one design constitutes an opportunity to develop advanced fiber reinforced composites in response to these challenges [5, 6].

Research on ballistic materials has explored multiple approaches to enhance their properties. Both Nurazzi et al. and Odesanya et al. [7, 8] studied natural fiber-reinforced polymer composites as an eco-friendly alternative to synthetic fibers like Kevlar. Despite the promise of these materials as energy absorbing, sustainable systems, their mechanical properties commonly do not meet the material constraints of high velocity ballistic protection. Composite metal foams (CMFs), along with ceramics and Kevlar, were identified by Garcia-

Avila et al. [9] as promising materials for high-performance lightweight armor systems. However, manufacturing costs and scalability are still challenges for these materials, which do not effectively absorb projectile energy and lower overall weight. Ceramic polymer composites studied by Colombo et al. and Klement et al. [10, 11] have shown exceptional penetration resistance in personal and vehicular applications. Lightweight protection can be provided from designs containing silicon carbide foams and polymer backings, which are useful for structural and vehicular defense. This is similarly the case with hybrid designs consisting of polymers with ceramics [12, 13], which demonstrate scalability over a range of projectile sizes, and performance superior over many hits. While they offer many benefits, ceramics are brittle and do not survive repeated impacts coming in, resulting in catastrophic failure; advanced reinforcement strategies are required. The most recent ballistic protection advancements have concentrated on combining high-performance fibers with advanced adhesives and innovative layer configurations. The role of high strength fibers like Kevlar, UHMWPE and polybenzoxazole (PBO) in increasing energy dissipation and tension strength was studied by He et al., and Cheeseman and Bogetti [14, 15]. Indeed, these materials have excellent energy absorption but need good bonding with the matrix for reduction in delamination and improved load transfer. According to the study by Zou

[16], innovations such as 3D printed armor and elements like graphene (carbon based and essentially carbon nanomaterial) offer large potential for lightweight, sustainable and protective systems. Yet such materials integration into scalable, cost-effective designs will remain a challenge.

The use of multi-layered composite structures is also explored, as they effectively balance strength, flexibility, and energy absorption, while incorporating material innovations. Štiavnický and Adamec [17], and Carpenter et al. [18] demonstrate in their research that layered configurations achieve effective dispersion of impact energy and increased durability. Strategically, these systems combine different materials, whose properties are complementary such as hard outer layers for penetration resistance and a softer inner layer for energy dissipation. This work is compatible with the principles of sustainable design described by Wantang et al. [19] and Radif et al. [20] by integrating natural fibers and bio-derived polymers in multi-purpose armor systems.

Several recent academic studies document the rising application of natural fiber hybrid composites which constitute environmental-friendly options instead of Kevlar synthetic fibers. The study by Devarajan et al. [21] conducted research on flax hemp jute fibers for body armor applications because of their energy dissipation capabilities combined with their lightweight composition. Their optimal mechanical capability requires further development. New ballistic composite performance improvements result from hybridization approaches. The study by Tai et al. [22] evaluated UHMWPE reinforced with carbon fibers leading to improved tensile strength alongside increased impact resistance which makes it suitable for protective usages. Babassu fiber-reinforced epoxy composites achieved higher tensile strength and impact performance when the composites contained 30% fiber volume according to Chaves et al. [23]. Dođru et al. [24] conducted research on basalt fiber-reinforced composites which proved that basalt fibers support increased impact resistance together with advanced flexural properties when used independently or with hybridization. The analysis demonstrates why hybrid composite structures remain essential because they manage to combine effective energy absorption capabilities with structural stability.

Based on these advancements, this study develops and examines two fiber reinforced composite models for lightweight ballistic protection. Model One consists of carbon, glass and Kevlar fibers bonded to a hybrid adhesive matrix consisting of natural rubber (NR), unsaturated polyester resin (UPS) and cornstarch. The same fiber configuration as Model Two is used with greater UPS content in the adhesive to improve stiffness and interfacial bonding. The impact resistance, hardness, tensile strength, compressive strength, and bending behavior of both models were systematically characterized. Real world performance was assessed by ballistic testing using 7.62×39 mm ammunition fired into TPU from a Kalashnikov (AK-47) rifle, while internal structural response was probed using X-ray imaging.

This study correlates mechanical properties to ballistic performance in order to determine the optimum body armor design for lightweight, cost-effective body armor. Furthermore, the possibility of hybrid design, the fusion of the best of both models is investigated, which leads to potential applications of new solutions in personal and mobile protective systems.

2. MATERIALS AND METHODS

2.1 Adhesive material

The adhesive formulations in this study were designed to ensure optimal bonding, durability, and impact resistance in composite structures. Two different formulations were prepared, each with specific proportions of unsaturated polyester resin (UPS), natural rubber (NR), and corn starch (CS) to evaluate their effect on ballistic performance.

UPS, sourced from Industrial Chemicals & Resins Co. Ltd (ICR), Saudi Arabia, was selected for its high-performance adhesion and compatibility with composite materials. This resin is a clear, viscous liquid with a density of 1.2 g/cm³ at room temperature. To enhance curing, methyl ethyl ketone peroxide (PMEK) was added as a catalyst at a ratio of 2 g per 100 g of UPS, allowing for controlled thermosetting.

To improve flexibility and energy absorption, natural rubber (MSR 10) from Al-Diwaniya Rubber Products Company was incorporated. Since rubber is initially in a solid state, it was dissolved in toluene (C₇H₈), a solvent obtained from Alpha Kimica, India, to convert it into a thick liquid phase, ensuring uniform dispersion within the adhesive.

Corn starch, supplied by Hashem Industry and Trading Group, Lebanon, was introduced into the adhesive to enhance adhesion properties and reduce costs while maintaining mechanical integrity.

Adhesive Formulations:

Two distinct adhesive formulations were prepared for comparative analysis:

- Model One Adhesive: 55% UPS, 25% CS, and 20% NR

- Model Two Adhesive: 75% UPS, 25% CS

These formulations were selected to examine the impact of UPS concentration on mechanical performance. Higher UPS content increases stiffness and interfacial bonding, while higher NR content enhances flexibility and energy dissipation.

2.2 Supporting materials

The materials selected for this study were chosen for their unique properties, which contribute to the overall performance of the composite armor. Kevlar fibers provide exceptional tensile strength and impact resistance, carbon fibers offer high stiffness and strength-to-weight ratios, and fiberglass adds durability and cost-efficiency. The stainless-steel mesh enhances structural reinforcement and energy dissipation under impact conditions.

Table 1. Specifications of Aramid Kevlar® 49 Used in Body Armor

Properties	Aramid Kevlar® 49
Density (g/cm ³)	1.44
Tensile Strength (MPa)	3000
Tensile Modulus (GPa)	112
Elongation at Break (%)	2.4
Temperature (°C)	25.0
Moisture Absorption (%)	3.5
Water Absorption (%)	3.5
Tenacity (N/tex)	2.08
Poisson's Ratio	0.36

To construct the composite layers, high-performance reinforcement materials were selected for their mechanical

properties and compatibility with the adhesive matrix. Kevlar fabric was procured from Songhan Plastic Technology Co., Ltd., Japan; carbon fibers from Fiber Glast Developments Corp., USA; and fiberglass from Sichuan Weibo New Material Group Co., Ltd., China. Expanded metal mesh (1.2 m × 10 m rolls) was sourced from Anping Shengsen Metal Wire Mesh Products Co., Ltd., China, to provide additional structural reinforcement. The properties of these materials are summarized in Tables 1-4.

Table 2. Specifications of carbon fiber used in body armor

Properties	Carbon Fiber
Tensile Modulus (dry)	33.0–41.5 MSI
Tensile Strength (dry)	700–850 KSI
Full Roll Length	100 yards
Color	Black
Modulus Fiber (min)	33.0 MSI
Tensile Strength (min)	700 KSI

Table 3. Specifications of fiberglass used in body armor

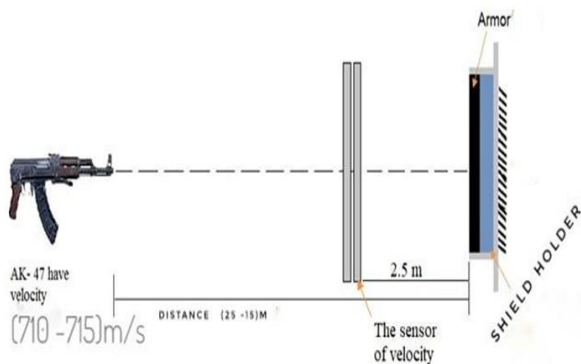
Product Code	Unit Weight (g/m ²)	Width (mm)	Length (m)
EW4000-1000	400 ± 32	1000 ± 10	100 ± 4

Table 4. Specifications of expanded metal mesh used in body armor

Material	Opening Width	Opening Length	Mesh Shape
Stainless Steel, Iron, Aluminum	0.3mm to 200mm	1mm to 4mm	Diamond/Hexagonal

2.3 Production of body armor

The fabricated body armor models, with their thickness and weights shown in Table 5, were tested according to the globally recognized NIJ-0101.06 standards. The testing involved firing 7.62×39 mm ammunition from a Russian-made Kalashnikov (AK-47) rifle at initial velocities ranging from 710 to 715 m/s. The tests were conducted at varying distances to evaluate the penetration resistance of each model. These tests were conducted at the Iraqi Police firing range with professional assistance from police personnel experienced in field training.



(a) Measurements of projectile velocity and secured armor sample are shown from a velocity sensor and shield holder, respectively



(b) Image of the 7.62×39 mm ammunition used in the ballistic tests

Figure 1. Schematic representation of the ballistic testing setup

Figure 1 (a) illustrates the setup for testing the ballistic armor at different distances. Figure 1(b) displays the 7.62×39 mm bullets used during testing, which were fired at initial velocities of 710-715 m/s.

Two body armor models were developed to enhance ballistic resistance and provide lightweight protection. Each armor sample measured 20 × 20 cm² and was designed to optimize impact resistance and energy absorption.

2.3.1 Model One

The first model consisted of six layers each of Kevlar fibers (KF), carbon fibers (CF), and glass fibers (GF), interspersed with 18 layers of stainless-steel mesh (CI) (see Figure 2). The mesh layers were distributed among the fiber layers, with six mesh layers between each fiber type. These layers were bonded using an adhesive comprising 55% UPS, 25% corn starch (CS), and 20% natural rubber (NR). Additionally, 48 layers of fiberglass were used without the inclusion of metal mesh. These layers were split into two groups of 24, forming the front and back plates, which were bonded with the same adhesive formulation.

2.3.2 Model Two

The second model utilized the same fiber configuration as Model One but with an adhesive formulation consisting of 75% UPS and 25% CS (see Figure 2). Stainless steel mesh and fiberglass configurations were maintained at their Model One levels except for the adhesive composition to study the effect of increased UPS content.

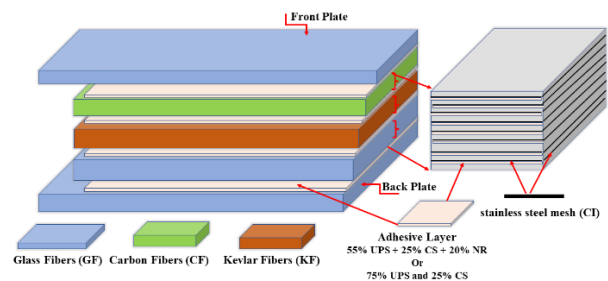


Figure 2. Cavity geometry

A hand lay-up process created composite layers by applying sequentially each prepared adhesive to individual specimens before stacking them in a 21 × 21 cm² mold. The laminated structure went through 28 hours of mechanical pressing using 10 MPa to achieve proper adhesive bonding and remove all air voids. The samples underwent room temperature thermal

curing at 27°C for three days to achieve complete adhesive matrix polymerization and stabilization.

Specifications of the prepared body armor samples are tabulated in Table 5.

Table 5. Specifications of prepared body armor samples

Sample	Materials Used	Layers	Layer Thickness (cm)	Total Thickness (cm)	Total Weight (g)
Sample 1,2	GF, KF, CI,	24, 6, 6,	1.344, 0.052,	± 3.056	2707
	CF, CI, GF,	6, 6, 6,	0.07, 0.05,		
	CI, GF	6, 24	0.07, 1.344		

2.4 Mechanical tests

2.4.1 Impact resistance and energy absorption analysis

Impact testing measures the energy absorbed by a material during fracture when subjected to high-velocity impacts. This test is crucial for evaluating the toughness and energy dissipation capabilities of materials under sudden loading [25-27]. The Izod Charpy Tension Impact Test was chosen to assess the composite's ability to absorb and dissipate kinetic energy, a key property for ballistic resistance.

Impact test samples were prepared with dimensions of 100 mm × 20 mm × 25 mm according to ASTM D6110 [28] for reinforced materials and 4 mm × 10 mm × 80 mm according to ISO-180 [29] for the adhesive material. Testing was performed using an Izod Charpy Tension Impact Testing Instrument by Testing Machines, Inc., USA. During the test, the sample was fixed in place, and a pendulum was released to strike and fracture the sample. The energy absorbed during fracture was recorded, with the hammer energy set at 7 J for the adhesive material and 300 J for the composite material.

2.4.2 Surface hardness and material toughness assessment

Hardness testing evaluates a material's resistance to surface indentation or penetration revealing some degree of durability and wear resistance. This study also utilized Shore–D hardness testing in order to test the adhesive and composite layers' ability to not be severely damaged by repeated impacts while retaining structural integrity.

The composite and adhesive samples were hardened hardness testing using a Shore-D Hardness Tester (Elcometer 120 Shore D) from Elcometer, UK. The samples were tested in accordance with international ASTM standards [ASTM-D 2240] [30]. To test the hardness of the sample, the surface had a needle shaped indenter penetrate it, and the value is read off on an internal gauge.

2.4.3 Tensile strength and elastic behavior evaluation

Evaluating the material's ability to resist forces that try to pull the material apart is what tensile testing does. This test gives the most important information of tensile strength, modulus of elasticity, and elongation at break characteristics that are useful when investigating strength and ductility of the composite. Selection of adhesive and composite materials for ballistic applications was based on tests to determine the load bearing capacity and flexibility of the adhesive and composite materials to insure suitability for ballistic applications.

Tensile test samples were prepared with standard dimensions of 150 mm × 20 mm × 25 mm according to ASTM D3039 [31] for reinforced materials and ASTM D638-22 [32] for the adhesive material. Testing was conducted at room

temperature using the LARYEE Yaur Testing Solution machine. Each sample was secured between the jaws to ensure stability during the test. Upon activation, the machine's grips applied tensile forces from both ends of the sample, stretching it until failure. The force-displacement data were used to generate stress-strain curves, from which tensile properties, including tensile strength, were calculated.

2.4.4 Compressive strength and deformation behavior

Compressive testing evaluates the material's ability to withstand forces that attempt to reduce its size. This test gives important information on compressive strength and deformation behavior, which are important to understand how composite layers respond to concentrated force in a ballistic impact. To make sure the materials could withstand high pressure conditions, compression tests were included.

Compression test samples were prepared with dimensions of 20 mm × 20 mm × 20 mm according to ISO 3384 for reinforced materials and ASTM D695 [33] for the adhesive material. Testing was conducted using the LARYEE Yaur Testing Solution machine from Laryee Technology Co., Ltd., China. Compressive strength was measured by applying a compressive load at a rate of 5 mm/min until failure. The results were obtained from the stress-strain curves generated during the test.

2.4.5 Flexural performance and structural integrity analysis

Bending tests, also known as flexural tests, measure the material's ability to resist deformation under a distributed load. This test evaluates flexural strength and stiffness, which are critical for determining how the composite behaves under dynamic loading conditions, such as those encountered during projectile impacts. The three-point bending test was selected to analyze the material's ability to maintain structural stability under bending forces.

Bending test samples were prepared with dimensions of 150 mm × 20 mm × 25 mm according to ASTM E290-22 [34] for reinforced materials and 100 mm × 8 mm × 3.5 mm according to ASTM D790-23 [35] for the adhesive material. The three-point bending test involved fixing the sample on two support points and applying a load at the midpoint. The resulting stress-strain curves, obtained from the testing machine, were used to calculate bending strength.

2.5 Mechanical tests

2.5.1 X-ray imaging analysis

X-ray imaging is a nondestructive testing method, which uses different density structure to visualize the internal structure of the material. The utilization of this method is vital to quantify bullet penetration into the thickness of the samples, deformation of layers, and structural integrity of the composite samples tested by ballistics. To validate the experimental findings, we chose x ray imaging which supplies detailed information on internal behavior of the samples.

The internal structure of the samples was analyzed and bullet penetration and residual positioning was assessed using x-ray imaging. Images were generated from internal details based on differences in material density without the destruction of the material. An X-ray beam was directed through the sample to a detector on the other side of the sample. The resulting image provided insights into the bullet's behavior, including its depth of penetration and whether it remained within the composite layers. The X-ray imaging

system used was manufactured by JPI, South Korea. The fabricated body armor models, as described earlier, were evaluated for their ballistic resistance under standardized field test conditions. The fabricated body armor models, with their thickness and weights shown in Table 5, were tested according to the globally recognized NIJ-0101.06 standards. This assessment highlights the effectiveness of the adhesive formulations and the reinforcement materials in resisting high-velocity impacts.

Five repeated tests of each mechanical testing method (tensile, compressive, bending, impact and hardness tests) involving five specimens per model were performed for statistical reliability. Ballistic field testing utilized three analogous samples from each model for validating the bullet resistance consistency when faced with actual conditions.

Means and standard deviations from the collected data enabled statistical analysis to determine direct measurement of repetition-based variability. The standard deviation (SD) measured dispersion levels for all mechanical tests while one-way ANOVA provided statistical confirmation about model differences.

3 RESULTS AND DISCUSSION

3.1 Impact test results

The impact resistance results (Table 6) demonstrate distinct differences between the adhesive materials and the complete composite structures of both models.

Table 6. Impact test results of two models

Model	Adhesive Material (kJ/m ²) (Mean ± SD)	Composite Structure (kJ/m ²) (Mean ± SD)
Model 1	0.075 ± 0.0045	145 ± 3.2
Model 2	0.0375 ± 0.0038	150 ± 2.9

The impact resistance of composite materials is a critical parameter, especially in applications such as body armor, where energy absorption and dissipation are vital for protection. Two composite models were assessed for their impact resistance, at both the adhesive material level and as a complete structure.

Model Two had an impact resistance of 0.0375 kJ/m² while Model One had 0.075 kJ/m². The nature of the adhesive formulation for Model One, explains the extra bit of elasticity in Model One's adhesive formulation and it works lead to superior performance as compared to finger stickers. It is well known that natural rubber has high elasticity and damping capacity to absorb and dissipate energy via internal damper mechanisms. NR incorporation improves the toughness of the adhesive by allowing dissipative energy mechanisms during simulated impact events that in turn enable the material to more readily resist crack initiation and propagation. Rubber toughening is a phenomenon that has been studied extensively for its effectiveness as a means to improve the impact resistance of polymer matrices [36-40].

On the other hand, Model Two's adhesive consists of a larger proportion of Unsaturated Polyester Resin (UPS), which leads to a stiffer matrix with limited energy dissipation capability. The inertia in the rigid UPS structure along with its inherent brittleness and the lower damping capacity render it

to absorb less impact energy at the adhesive level. Flexible components, such as NR, have been shown to enhance impact resistance, by promoting energy dissipation mechanisms, when incorporated into a rigid polymer matrix [41].

When considering the entire composite structures, the impact resistance exhibited a higher value for Model Two, estimated at 150 kJ/m² in comparison with 145 kJ/m² for Model One. Model Two was shown to exhibit an improved interfacial bonding due to greater UPS content in this model resulting in improved performance. An effective load transfer and uniform stress distribution within the composite is ensured by strong adhesion between the UPS matrix and reinforcing fibers (Kevlar, carbon, and glass) and between the stainless-steel mesh and the UPS matrix. In composite materials, effective interfacial bonding is mandatory, as it averts delamination and fiber pullout under impact loading and hence increases the impact resistance of the material. Significant improvements in the mechanical performance of composites have been demonstrated as a result of research which optimized the interfacial adhesion between the matrix and reinforcement phases [42].

Model Two exhibits a small advantage in overall impact resistance, due to its higher UPS content which compensates for the poorer impact resistance of the adhesive material, but provides superior interfacial bonding and structural cohesion. Intimately related to this finding is the importance of taking into account the intrinsic adhesive properties as well as the interfacial interactions within the composite structure when designing materials for impact resistance applications.

3.2 Hardness test results

Table 7 results from the hardness tests, show how the adhesive materials and the fiber reinforced composite structure contribute to surface resistance.

Table 7. Hardness test results of two models

Model	Adhesive Material (N/mm ²) (Mean ± SD)	Composite Structure (N/mm ²) (Mean ± SD)
Model 1	77 ± 2.1	97.7 ± 1.8
Model 2	79.4 ± 2.4	97.7 ± 1.5

The hardness of composite materials is an important property determining its wear resistance and durability in the case of using under mechanical contact and surface abrasion. In this work, we tested two models of composites using hardness tests and analyzed how much of the measured values is due to the fiber reinforced structures and how much is due to the adhesive materials.

For Model One, the adhesive material showed a hardness value of 77 N/mm² while Model Two showed a higher hardness value of 79.4 N/mm². The difference between the two is primarily caused due to the high cross-linking density of the UPS adhesive in Model Two's adhesive formulation. A more rigid, tightly bonded polymer network is obtained, increasing the material's resistance to localized deformations under indentation, at a higher cross link density. This type of relationship between cross-linking density and hardness is well recognized in polymer science: an increase in cross-linking leads to greater hardness and stiffness [43].

By contrast, the adhesive of Model One utilizes Natural rubber (NR) which, in improving the elasticity and impact

resistance, may lower the overall cross-linking density and hardness of the adhesive matrix. The presence of NR thus added flexible segments to the polymer network and could potentially decrease the hardness via increased molecular mobility. However, a tradeoff between flexibility and hardness is often desired for polymer composites, when toughening through the addition of elastomers at the expense of surface hardness is sought.

The structural level coefficient of hardness of both composite models was identical at 97.7 N/mm². Observation: The hardness of the complete composite is led by the reinforcing fibers and the stainless-steel mesh, and is not the adhesive matrix. A rigid and robust framework is formed by Kevlar, carbon, and glass fibers, and stainless-steel mesh, that dictate the surface hardness of the composite. Hardness of fiber reinforced composites have values commonly significantly influenced by the type, orientation and volume fraction of the reinforcing fibers. In the current case, the same fiber architecture in both models produce roughly the same hardness measurements, overriding the differences in the adhesive materials [44-46].

This result is consistent with other studies which show that the matrix material makes a small contribution to the overall mechanical properties, while the reinforcement phase contributes significantly to surface hardness. For instance, it has been shown that adding hard fillers or fibers into a matrix polymer gives a great increase in composite hardness, while the effect of matrix material becomes smaller with higher reinforcement content [47-49].

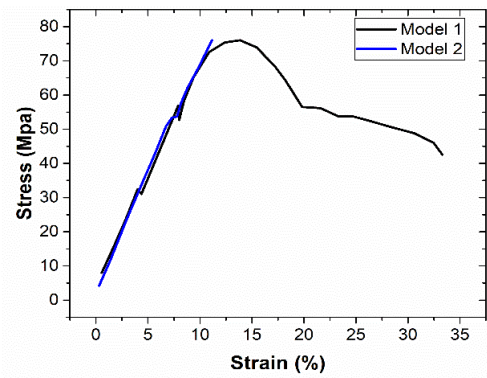
3.3 Tensile test results

The tensile properties of the two composite models: elastic modulus, ultimate tensile strength and ductility were assessed via stress-strain analysis Figure 3 (a). The study results show how the adhesive matrices, fiber reinforcements, and strategic placement of front and back glass fiber layers contribute to the mechanical performance of the composites.

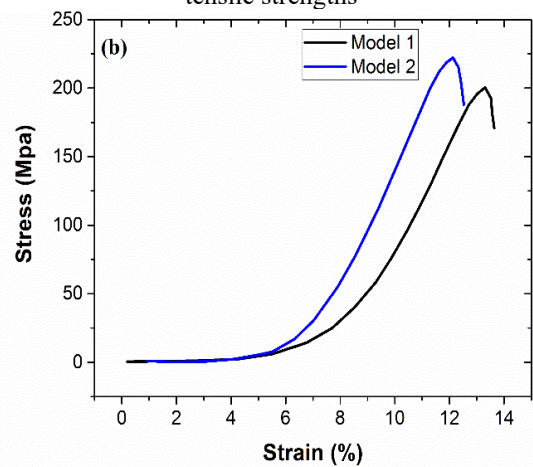
Model One had a slightly lower Young's modulus of 6.77 MPa than Model Two's 7.37 MPa, which corresponded to greater stiffness. The higher unsaturated polyester resin (UPS) content in Model Two's adhesive matrix forms a dense cross linked polymer network, restricting molecular mobility and increasing resistance to elastic deformation, and this is primarily responsible for Model Two's increased stiffness. Carbon fibers also contribute rather significantly to stiffness. Carbon fibers with their highly aligned graphene microstructure lend significant rigidity and load bearing capacity with tensile modulus optimized for the lightest weight composite [50]. Also, due to its stiffness intrinsic in the Kevlar fibers and that resulting from the glass fibers reinforcement, the composite shows a better potential to resist deformation also under axial tensile forces [51].

The two models achieved an identical ultimate tensile strength of 76.05 MPa, suggesting that the performance of the reinforcement fibers, and to a lesser extent, stainless steel mesh (CI) dictated the maximum tensile capacity. The inclusion of Kevlar fibers increases the tensile strength by their loadbearing capacity and resistance to crack propagation. In addition, the carbon fiber further enhances the performance of the composite, giving excellent fatigue resistance and strength retention under cyclic loading. In addition, glass fibers possess balanced mechanical properties and are used to complement Kevlar and carbon fibers as a source of strength. Stress

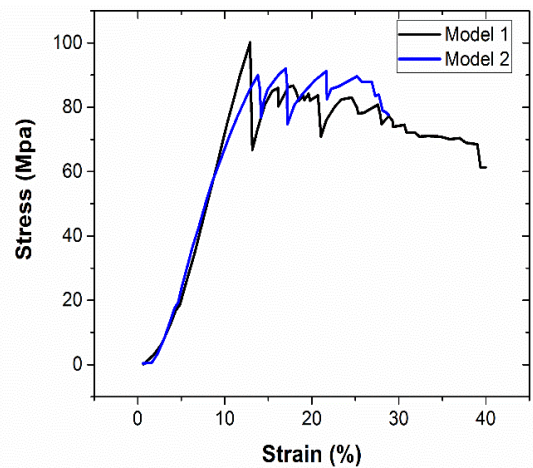
concentrations are mitigated by strategic placement of 24 layers of glass fibres at the front and back of the composites. The front layers receive initial axial loads, and the back layers are used to stabilize the structure preventing delamination, more uniform stress distribution.



(a) Tensile test, showing elastic-plastic behavior and ultimate tensile strengths



(b) Compressive test illustrating material behavior responding to axial compression to failure



(c) Bending test, illustrating flexural performance and maximum bending stresses

Figure 3. Stress-strain curves of two models for various mechanical tests

Model One proved to have ductility, with a significantly higher fracture strain of 33.3%, 3 times higher than 11.16% for Model Two. The higher natural rubber (NR) content in the adhesive matrix of Model One provides an explanation for this

enhanced ductility. Flexible elastomeric segments are introduced into a matrix in NR and can absorb energy and allow large deformation before failing. A secondary reinforcement mechanism involving strain induced crystallization of NR under the drawn loads helps to improve the toughness and retard the crack propagation. However, the higher UPS content leads to a stiffer adhesive matrix in Model Two, limiting chain mobility and plastic deformation, which in turn limits ductility and results in earlier failure.

3.4 Compressive test results

The results of the behavior of the two composite models under axial compression (Figure 3 (b)) are indicated by the presented compressive stress-strain curves. Mechanical performance of adhesively reinforced thermoplastic composites was evaluated through key parameters such as compressive modulus, compressive strength, and ductility, to illustrate the reinforcing fibers and adhesive matrices' influence on different mechanical properties.

Model Two had a higher compressive modulus of 0.41 MPa compared to 0.21 MPa in Model One and was thus stiffer in the elastic region. The increased stiffness is predominantly accounted for by the higher crosslinking density of the adhesive matrix of Model Two leading to its resultant higher amount of unsaturated polyester resin (UPS). The UPS matrix exhibits enhanced resistance to initial deformation under compressive loads due to the modification of molecular motion by a dense crosslinked network. In addition, this property is quite suitable in some applications where structural stability and rigidity is needed under axial forces [52].

Further, due to the high modulus and ability to withstand compressive loads without buckling (on the fiber scale), carbon fibers also contribute significantly to stiffness. Furthermore, the glass fibers in the front and back layers confer additional resistance against deformation, sparing it by uniformly distributing its compressive forces, as well as strengthening the overall structure of the composite.

Model Two showed better compressive strength, of 222.07 MPa, than Model One with 200.53 MPa. Improved interfacial bonding between the adhesive matrix and reinforcing fibers results in the higher compressive strength. It therefore guarantees efficient load transfer across the composite which minimizes localized failure under axial compression.

Kevlar fibers are characterized with high compressive strength and toughness, which greatly contributes to increase the load-bearing capacity of both models. Under compressive stress these fibers resist buckling and cracking, enhancing the composites' ability to carry high loads. By stabilizing the composite and preventing localized deformation, the stainless-steel mesh (CI) prevents localized deformation and uniformizes the compressive forces applied.

Model One showed a slightly higher fracture strain (13.64%) than Model Two (12.53), which implies higher plastic deformation capacity before failure. The higher content of natural rubber (NR) in the adhesive matrix of Model One is responsible for this enhanced ductility. NR provides a flexibility to the material and the material can absorb energy and undergo plastic deformation without cracking or fracturing. NRs elastomeric nature creates an ability of energy dissipation during compression with a delay to the onset of failure.

Conversely, Model Two has a higher content of UPS and as a result a stiffer adhesive matrix which increases compressive

strength but reduces the ability of the material to deform plastically. The decreased ductility of Model Two is associated with the lower mobility of polymer chains within its crosslinked network, which prevents the absorption and redistribution of energy through deformation.

3.5 Bending test results

The flexural behavior of the two composite models is well described by the bending stress-strain curves (Figure 3 (c)). The results reveal the effects of adhesive matrix, reinforcing fibers and composite structural configuration on the composite bending performance.

Model One had a higher bending modulus of 3.88 MPa compared to 3.14 MPa for Model Two, demonstrating higher stiffness in the elastic region. The adhesive matrix of Model One with natural rubber (NR) encased in the polyurethane structure results in improved elastic properties and thus higher modulus. The NR component provides for flexibility and energy absorption in the beginning stages of the bending process, reduces the stress concentrations, and provides a more uniform load distribution.

The bending modulus is contributed from the reinforcing fibers also. The glass fibers, located in the front and back layers, are very critical to resist bending deformation. In order to maintain the shape of the composite structure under bending loads, the composite structure has high flexural stiffness in complement with the elastic matrix of the adhesive. Moreover, as the Kevlar fibers of the composite core provide toughness and energy dissipation capabilities, carbon fibers contribute to stiffness and deformation reduction [53, 54].

Model Two obtained a lower maximum bending stress of 92.02 MPa while Model One acquired a higher maximum bending stress of 100.16 MPa, signifying that the former is capable of enduring greater loads until failure. In Model One, the adhesive matrix consisting of natural rubber (NR) and unsaturated polyester resin (UPS) give this enhanced performance by providing more flexibility and energy absorption so that failure is delayed as much as possible under flexural loads.

The bending strength is greatly attributed to the melding of Kevlar fibers which are famous for its high tensile and compressive strength and carbon fibers with its excellent stiffness and load bearing capability. In these structures these fibers work in concert with the adhesive matrix to spread bending stresses uniformly over the structure [55]. The composite's flexibility and energy absorption are further improved through the use of glass fibers, and stainless-steel mesh (CI) provides stabilization to the structure to retain its integrity under high flexural loads.

A much higher fracture strain of 39.97% was observed for Model One compared to 28.8% for Model Two, demonstrating greater ductility when bending loads are exerted. Model One has higher ductility than the other three because the higher NR content in its adhesive matrix affords greater plastic deformation prior to fracture. NR being elastomeric can dissipate energy through internal friction, and hence helps the composite to dissipate more energy than earlier when bent.

However, Model Two's adhesive matrix with higher UPS content demonstrates greater stiffness and reduced plasticity. Under bending loads, the dense cross-linked network of UPS restricts the molecular mobility to make mechanical failure earlier. In composite materials, the stiffness-ductility tradeoff is a well-known phenomenon; increasing matrix rigidity is

often accompanied by reduced flexibility and energy absorption.

3.6 Correlation between mechanical properties and suitability for body armor

Impact, hardness, tensile, compressive and bending tests are performed on the composite models to obtain its mechanical properties, which offers important knowledge of the behavior of the composite models. A fundamental understanding of the interdependencies among these properties is necessary to clarify their suitability for lightweight and effective body armor. We discuss below the relationships between these mechanical quantities, and to what extent each of these quantities is relevant for each model.

3.6.1 Model One

The higher ductility and energy absorption capabilities of Model One characterize its mechanical behavior. Its adhesive hardness is in fact lower than Model Two (77 N/mm²) and its adhesive material has the capacity to resist impact (energy absorbed: 0.075 kJ/m²) significantly higher than Model Two. The higher natural rubber (NR) content in the adhesive matrix of Model One results in this trade off. The NR imparts elasticity to the material for better energy dissipation during impact at the expense of slightly lower surface stiffness and resistance to localized deformation.

This is confirmed by the tensile properties as well. The model One displayed improved ductility, requiring a fracture strain of 33.3% as against 11.16% for model Two. This aligns with the material's ability to deform elastically (without fracture) under tensile loading and absorb energy in the process. Similarly, the compressive properties of Model One is a result of its capability to sustain plastic deformation and fracture at a strain of 13.64%, which is expectedly higher than Model Two (12.53%). These results imply that Model One can absorb large amounts of energy under both tensile and compressive stresses, both important defeats for mitigating the impact of ballistic events.

Flexibility is observed in the bending of Model One, shown by a fracture strain 39.97% and a bending modulus of 3.88 MPa. With these values, a large amount of deformation can be seen before failure, thereby extending the material's ability to avoid local flexural loading from concentrating on small areas. This behavior agrees with its tensile and compressive performance, and demonstrates that the material experience a cohesive behavior under different loading conditions. Model One combined high ductility, impact resistance, and flexibility for applications requiring considerable energy absorption and adaptability, including intermediate or backing layers in body armor.

3.6.2 Model Two

The higher stiffness and strength across several mechanical tests distinguish Model Two's performance. Model Two (150 kJ/m²) is more impact resistant structurally compared with Model One (145 kJ/m²), consistent with its greater hard adhesive (79.4 N/mm²). Model Two's adhesive matrix with a higher UPS content has increased cross-linking density, creating a stiffer and more rigid material that resists localized deformation and transfers impact energy over a larger area. Such property is of paramount importance for primary ballistic protection layers of body armor, where strength and structural integrity are required.

Tensile tests also point to the stiffness of Model Two with higher Young's modulus (7.37 MPa) than Model One (6.77 MPa). Although it has similar tensile strength (76.05 MPa) compared to Model One, the lower fracture strain (11.16%) means lower deformation capacity. The tradeoff in this material can be described as one optimized for rigidity and stretching forces than flexibility. Similar trends for compressive behavior are observed as Model Two showed better compressive strength (222.07 MPa), stiffness (0.41 MPa), but slightly less ductility (12.53% fracture strain). In light of the resulting compressive stiffness of Model Two greater than that of Model One, these results suggest that Model Two is better suited for resisting high stress compressive forces, as those caused by typical ballistic impact.

Model Two performs in tensile and compressive as it does in bending. Its ability to withstand higher flexural loads is reflected in a maximum bending stress of 92.02 MPa as compared to Model One. However, the lower bending fracture strain (28.8%) illustrates its impact on the system's flexibility under bending loads. These results highlight Model Two's affinity for structural rigidity rather than energy absorption and indicate Model Two's suitability for use in load bearing and protective applications where deformation must be minimized.

3.7 Cross-property correlations

The mechanical properties of Model One and Model Two exhibit interplay, and accordingly each model contributes a set of complementary properties in body armor design. Model One's superior adhesive level impact resistance is consistent with its higher ductility in tensile, compressive, and bending tests and it is therefore able to effectively absorb and dissipate energy. Such properties also make it a strong candidate for applications that require both flexibility as well as energy absorption. However, the superior structural impact resistance, tensile stiffness, compressive strength, and bending strength of Model Two is representative of a material seeking to be as rigid and able to provide support as possible. The features are needed in primary ballistic protection layers in which strength and structural integrity are so important.

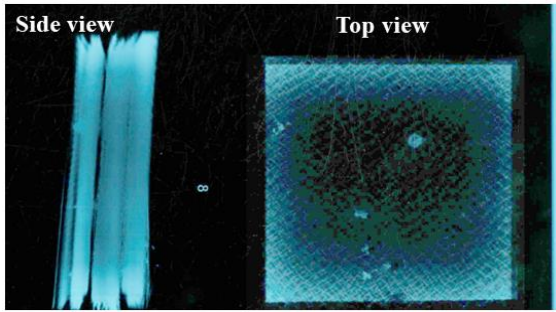
3.8 Field ballistic testing and analysis

The performance difference between the two models was explicitly shown. At 23 meters Model One did not resist penetration, suggesting poorer ballistic resistance. By comparison, Model Two withstood penetration at the same distance, proving that its structural integrity and the impact resistance under high-velocity conditions were superior. Its mechanical properties, as detailed below, have a strong correlation with the superior ballistic performance of Model Two.

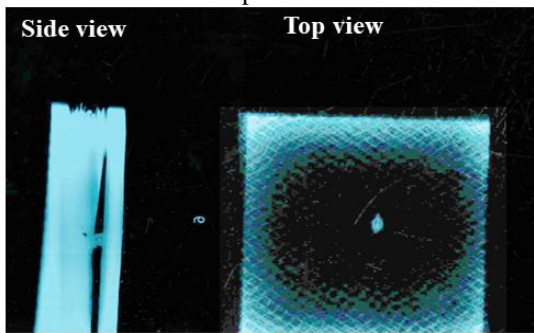
3.9 X-ray imaging results

Structural response of Model One and Model Two to ballistic impacts was assessed via X-ray imaging, allowing for the detailed side and top profile view of both Models One and Two (see Figure 4 (a) and (b)). Imaging showed that bullets did not penetrate through both models' composite layers at the tested distances. Conversely, the projectiles were compatible inside the layers of the composite, illustrating the ability of

both models to absorb and breach the energy of high velocity impacts without complete penetration.



(a) Model One shows visible damage propagation in the layers and retention of the projectile without complete penetration



(b) Model Two is an enhanced structural configuration demonstrating limited damage and containment of the projectile within the composite layers

Figure 4. X-ray imaging of ballistic test samples showing side and top views of the composite armor after impact

Model one is able to confine the projectile in composite layers due to higher ductility and ability to absorb more energy. Natural rubber in the adhesive matrix greatly to the flexibility and plastic deformation of layers where the kinetic energy of bullet was efficiently dissipated. Not only did the interspersed fiber reinforcements and stainless-steel mesh layers act as structural barriers, which are responsible for impacting energy redistribution as well as preventing complete penetration. These mechanical testing results are consistent with this structural behavior, and demonstrate Model One's better energy absorption properties under dynamic loading compared to traditional models of GG.

Model two shows greater structural rigidity and more interfacial bonding and provides the capability to contain the projectile within the composite structure. An increase in the content of unsaturated polyester resin (UPS) in the adhesive matrix enabled increased stiffness, cohesion and delamination behavior of layers, which allowed the effective load transfer and energy distribution during the impact. The structure was also reinforced by the stainless-steel mesh layers, which effectively created a grid which then absorbed and redirected the projectile's energy. The layers of Kevlar and carbon fiber imparted some resistance to penetration to the composite, and maintained structural integrity even under high stress conditions.

Ballistic testing and mechanical evaluations are complemented by the X-ray imaging results. The bullets remain confined to the composite layers in both models, and thus, these designs can be considered robust from ballistic protection standpoint. The ability to trap projectiles within the

material rather than having backface deformation or shattering the material (and thus causing secondary fragments) is a major advantage for personal protective use of a material where impact velocity is relatively high.

The X-ray images are however very significant since it shows a layered design of the rock. The composite structure in both models dispersed the energy of the bullet effectively, preventing catastrophic failure. The images on the side view definitely demonstrate how the layered architecture did prevent the impact forces from breaking the design apart, but rather distributed the impact forces amongst many layers and thus increasing resilience. Structural response of both models validates their design in mitigating ballistic threats.

Further support for this model of a hybrid design with strengths of two models is provided by these results. Model One has excellent ductility and energy absorption capabilities such that these can be used to mitigate shock and dissipate energy; while Model Two has high stiffness and penetration resistance that ensures structural integrity. The most optimal design could be a hybrid configuration with a Model Two dominated structure with Model One placed as the intermediate layer for increased protection and energy absorption.

Complementary to the mechanical and ballistic testing data, the X-ray imaging results indicate that these composite materials are likely suitable for use in body armor. Future studies could extend these results to include multi-hit performance and durability under a variety of ballistic conditions. Further insights into the internal damage mechanisms and energy dissipation pathways could also be gained through the incorporation of advanced imaging techniques and used to improve these designs for improved performance.

In addition, SEM imaging at high resolution was not possible for our large-scale composite models although we analyzed microstructure-property relationships using theoretical frameworks together with mechanical performance correlations and similar composite study findings. Previous SEM research on fiber-reinforced polymer composites has revealed important findings about fiber-matrix bonding and detailed pathways of cracking as well as energy reduction methods [56]. The ballistic protection studies [57] reveal that the improved delamination resistance and impact absorption performance of Kevlar and carbon fiber composites stems from their three-dimensional woven structure.

Fracture examinations at the macroscopic level have been used to understand the behavior of fiber-matrix interactions and deformation patterns as well as crack propagation ways since direct SEM imaging was not available. X-ray imaging evidence highlights the ability of composites to retain bullets which demonstrates effective adhesive strength and energy dispersement between multiple reinforcement layers. The boundaries between stainless-steel mesh and Kevlar-carbon fiber interfaces served as crucial components in distributing impact energy in agreement with well-established failure models of hybrid fiber-reinforced composites. The study results validate how hierarchical reinforcement designs in ballistic-resistant materials make them ideal for body armor use.

4. CONCLUSIONS

This development and assessment of two lightweight ballistic composite models utilizing fiber-reinforced composites is shown to be successful due to their unique

mechanical and structural properties. As displayed in the above results, model one, containing more natural rubber, showed the highest ductility and energy absorption properties that made the model very efficient in dissipating the kinetic energy during high velocity impact. On the contrary, Model Two having higher unsaturated polyester resin content led to higher stiffness, compressive strength and tensile modulus that increased penetration resistance and structural integrity.

Field ballistic testing verified the practical effectiveness of both models as no complete penetration of the bullets through the composite layers was observed and bullets were confined inside composite layers. These findings are also validated by X-ray imaging which shows structural resilience of the composites under extreme conditions. Kevlar, carbon, and glass fibers in combination with stainless steel mesh reinforcements played a critical role in realizing these outcomes and in generating the layered architecture.

Additionally, the study shows the possibility of hybrid configurations utilizing the ductility and energy absorption of Model One as intermediate layers and the rigidity and penetration resistance of Model Two for outer layers. These designs could provide an optimal performance compromise between flexibility and protection as a complete solution for personal and vehicular ballistic armour.

These findings highlight the viability of natural rubber, corn starch, and unsaturated polyester resin combination formulations in adhesive systems, complemented with appropriate selection of reinforcement materials, to deliver low cost and high-performance composite systems. Further work could involve characterization of multi hit performance, long term durability, and scalability of these materials to open the door to their application in future advanced ballistic protection systems that can defeat short range threats and possibly rockets and other indirect fire. In addition, Additional Thermogravimetric Analysis (TGA) and Differential Scanning Calorimetry (DSC) analytical studies regarding adhesive matrix thermal stability will be conducted under high-speed impact to better understand heat-degradative processes while maximizing composite performance.

REFERENCES

- [1] Fonseca, V.M., Oliveira, E.J.P.A., Lima, P.T., Carvalho, L.H. (2018). Development of Kevlar composites for ballistic application. In 4th Brazilian Conference on Composite Materials, Rio de Janeiro, pp. 548-553. <https://doi.org/10.21452/bccm4.2018.09.04>
- [2] Monteiro, S.N., Drelich, J.W., Lopera, H.A.C., Nascimento, L.F.C., et al. (2019). Natural fibers reinforced polymer composites applied in ballistic multilayered armor for personal protection—An overview. In *Green Materials Engineering*, pp. 33-47. https://doi.org/10.1007/978-3-030-10383-5_4
- [3] Naveen, J., Jayakrishna, K., Hameed Sultan, M.T.B., Amir, S.M.M. (2020). Ballistic performance of natural fiber based soft and hard body armour-A mini review. *Frontiers in Materials*, 7: 608139. <https://doi.org/10.3389/fmats.2020.608139>
- [4] Bhatnagar, A. (2018). 3.19 Lightweight fiber-reinforced composites for ballistic applications. *Comprehensive Composite Materials II*, 3: 527-544. <https://doi.org/10.1016/B978-0-12-803581-8.09932-X>
- [5] Costa, U.O., Nascimento, L.F.C., Garcia, J.M., Monteiro, S.N., Luz, F.S.D., Pinheiro, W.A., Garcia Filho, F.D.C. (2019). Effect of graphene oxide coating on natural fiber composite for multilayered ballistic armor. *Polymers*, 11(8): 1356. <https://doi.org/10.3390/polym11081356>
- [6] Luz, F.S.D., Garcia Filho, F.D.C., Oliveira, M.S., Nascimento, L.F.C., Monteiro, S.N. (2020). Composites with natural fibers and conventional materials applied in a hard armor: A comparison. *Polymers*, 12(9): 1920. <https://doi.org/10.3390/polym12091920>
- [7] Nurazzi, N.M., Asyraf, M.R.M., Khalina, A., Abdullah, N., et al. (2021). A review on natural fiber reinforced polymer composite for bullet proof and ballistic applications. *Polymers*, 13(4): 646. <https://doi.org/10.3390/polym13040646>
- [8] Odesanya, K.O., Ahmad, R., Jawaid, M., Bingol, S., Adebayo, G.O., Wong, Y.H. (2021). Natural fibre-reinforced composite for ballistic applications: A review. *Journal of Polymers and the Environment*, 29(12): 3795-3812. <https://doi.org/10.1007/s10924-021-02169-4>
- [9] Garcia-Avila, M., Portanova, M., Rabiei, A. (2015). Ballistic performance of composite metal foams. *Composite Structures*, 125: 202-211. <https://doi.org/10.1016/j.compstruct.2015.01.031>
- [10] Colombo, P., Zordan, F., Medvedovski, E. (2006). Ceramic-polymer composites for ballistic protection. *Advances in Applied Ceramics*, 105(2): 78-83. <https://doi.org/10.1179/174367606X84440>
- [11] Klement, R., Krestan, J., Rolc, S. (2009). Ceramic materials for ballistic protection. *Key Engineering Materials*, 409: 291-294. <https://doi.org/10.4028/www.scientific.net/KEM.409.291>
- [12] Naebe, M., Sandlin, J., Crouch, I., Fox, B. (2013). Novel polymer-ceramic composites for protection against ballistic fragments. *Polymer Composites*, 34(2): 180-186. <https://doi.org/10.1002/pc.22397>
- [13] Hu, P., Cheng, Y., Zhang, P., Liu, J., Yang, H., Chen, J. (2021). A metal/UHMWPE/SiC multi-layered composite armor against ballistic impact of flat-nosed projectile. *Ceramics International*, 47(16): 22497-22513. <https://doi.org/10.1016/j.ceramint.2021.04.259>
- [14] He, Y., Jiao, Y., Zhou, Q., Chen, L. (2021). Research progress on ballistic response of advanced composite for ballistic protection. *Acta Materiae Compositae Sinica*, 38, 1331-1347. <https://doi.org/10.13801/j.cnki.fhclxb.20201201.004>
- [15] Cheeseman, B.A., Bogetti, T.A. (2003). Ballistic impact into fabric and compliant composite laminates. *Composite structures*, 61(1-2): 161-173. [https://doi.org/10.1016/S0263-8223\(03\)00029-1](https://doi.org/10.1016/S0263-8223(03)00029-1)
- [16] Zou, W. (2024). Recent advancements in ballistic protection—A review. *Journal of Student Research*, 13(1): 5936. <https://doi.org/10.47611/jsrhs.v13i1.5936>
- [17] Štiavnický, M., Adamec, N. (2015). Improved ballistic protection of vehicles using composites. In *International Conference on Military Technologies (ICMT) 2015*, Brno, Czech Republic, pp. 1-6. <https://doi.org/10.1109/MILTECHS.2015.7153750>
- [18] Carpenter, A.J., Chocron, S., Scott, N.L., Anderson Jr, C.E. (2023). Characterization, modeling, and ballistic impact of kevlar/phenolic PVB composite. *Journal of Dynamic Behavior of Materials*, 9(2): 225-239. <https://doi.org/10.1007/s40870-023-00376-9>

- [19] Wantang, T., Pipathattakul, M., Wiwatwongwana, F. (2023). Sustainable innovation in ballistic vest design: Exploration of polyurethane-coated hemp fabrics and reinforced sandwich epoxy composites against 9 mm and 40 S&W bullets. *Journal of Metals, Materials and Minerals*, 33(4): 1830-1830. <https://doi.org/10.55713/jmmm.v33i4.1830>
- [20] Radif, Z. S., Ali, A., Abdan, K. (2011). Development of a green combat armour from rame-kevlar-polyester composite. *Pertanika Journal of Science & Technology*, 19(2): 339-348.
- [21] Devarajan, B., Lakshminarasimhan, R., Murugan, A., Rangappa, S.M., Siengchin, S., Marinkovic, D. (2024). Recent developments in natural fiber hybrid composites for ballistic applications: A comprehensive review of mechanisms and failure criteria. *Facta Universitatis, Series: Mechanical Engineering*, 22(2): 343-383. <https://doi.org/10.22190/FUME240216037D>
- [22] Tai, J., Wu, C., Han, G., Sun, D., Zhao, G., Chen, Q., Liu, Y. (2024). Study on ballistic penetration behavior of unidirectional UHMWPE/carbon fiber composites: Experiments and numerical modeling. *Polymer Composites*. <https://doi.org/10.1002/pc.29433>
- [23] Chaves, Y.S., Monteiro, S.N., Nascimento, L.F.C., Rio, T.G.D. (2024). Mechanical and ballistic properties of epoxy composites reinforced with babassu fibers (*Attalea speciosa*). *Polymers*, 16(7): 913. <https://doi.org/10.3390/polym16070913>
- [24] Doğru, M.H., Yeter, E., Göv, İ., Göv, K. (2024). Ballistic impact resistance and flexural performance of natural basalt fiber with carbon and glass fibers in inter-ply hybrid composites. *Polymer Composites*, 45(11): 9785-9801. <https://doi.org/10.1002/pc.28438>
- [25] Ibraheem, E.K., Bdaiwi, W. (2024). Enhancing mechanical and thermal properties of unsaturated polyester composites through Sidr leaves' particle reinforcement. *Revue des Composites et des Matériaux Avances*, 34(3): 269-275. <https://doi.org/10.18280/rcma.340301>
- [26] Hameed, S.N., Salih, W.B. (2023). Enhancing mechanical and thermal properties of unsaturated polyester resin with luffa fiber reinforcements: A volumetric analysis. *Journal of Composite & Advanced Materials/Revue des Composites et des Matériaux Avancés*, 33(6): 357-362. <https://doi.org/10.18280/RCMA.330602>
- [27] Awad, S.K., Bdaiwi, W. (2024). Enhancing mechanical performance of PMMA resin through cinnamon particle reinforcement. *Revue des Composites et des Matériaux Avances*, 34(3): 379-384. <https://doi.org/10.18280/rcma.340313>
- [28] ASTM D6110-18. (2018). Standard test methods for determining the Charpy impact resistance of notched specimens of plastics. <https://www.astm.org/d6110-18.html>.
- [29] Standard, B., ISO, B. (2001). Plastics-Determination of Izod impact strength. http://www.hengyudg.com/Attachment/month_1403/201403100919127725.pdf.
- [30] ASTM D2240-15. (2021). Standard test method for rubber property—Durometer hardness. <https://www.astm.org/d2240-15r21.html>.
- [31] ASTM D3039/D3039M-08. (2014). Standard test method for tensile properties of polymer matrix composite materials. https://www.astm.org/d3039_d3039m-08.html.
- [32] ASTM D638-14. (2022). Standard test method for tensile properties of plastics. <https://www.astm.org/d0638-14.html>.
- [33] ASTM D695-23. (2023). Standard test method for compressive properties of rigid plastics. <https://www.astm.org/d0695-23.html>.
- [34] ASTM E290-14. (2022). Standard test methods for bend testing of material for ductility. <https://www.astm.org/e0290-14.html>.
- [35] ASTM D790-17. (2017). Standard test methods for flexural properties of unreinforced and reinforced plastics and electrical insulating materials. <https://www.astm.org/d0790-17.html>.
- [36] Okamoto, Y., Miyagi, H., Uno, T., Amemiya, Y. (1993). Impact toughening mechanisms in rubber - dispersed polymer alloy. *Polymer Engineering & Science*, 33(24): 1606-1610. <https://doi.org/10.1002/pen.760332404>
- [37] Bain, E.D., Knorr, D.B., Richardson, A.D., Masser, K.A., Yu, J., Lenhart, J.L. (2016). Failure processes governing high-rate impact resistance of epoxy resins filled with core-shell rubber nanoparticles. *Journal of Materials Science*, 51, 2347-2370. <https://doi.org/10.1007/s10853-015-9544-5>
- [38] Hassan, A., Haworth, B. (2006). Impact properties of acrylate rubber-modified PVC: Influence of temperature. *Journal of Materials Processing Technology*, 172(3): 341-345. <https://doi.org/10.1016/j.jmatprotec.2005.07.015>
- [39] Bagheri, R., Marouf, B.T., Pearson, R.A. (2009). Rubber-toughened epoxies: A critical review. *Journal of Macromolecular Science®, Part C: Polymer Reviews*, 49(3): 201-225. <https://doi.org/10.1080/15583720903048227>
- [40] Walker, I., Collyer, A.A. (1994). Rubber toughening mechanisms in polymeric materials. In *Rubber Toughened Engineering Plastics*, pp. 29-56. https://doi.org/10.1007/978-94-011-1260-4_2
- [41] Mastalygina, E., Varyan, I., Kolesnikova, N., Gonzalez, M.I.C., Popov, A. (2020). Effect of natural rubber in polyethylene composites on morphology, mechanical properties and biodegradability. *Polymers*, 12(2): 437. <https://doi.org/10.3390/polym12020437>
- [42] Jiang, D., Xing, L., Liu, L., Yan, X., et al. (2014). Interfacially reinforced unsaturated polyester composites by chemically grafting different functional POSS onto carbon fibers. *Journal of Materials Chemistry A*, 2(43): 18293-18303. <https://doi.org/10.1039/C4TA04055D>
- [43] Davallo, M., Pasdar, H., Mohseni, M. (2010). Mechanical properties of unsaturated polyester resin. *International Journal of ChemTech Research*, 2(4): 2113-2117.
- [44] Sharma, M., Rao, I.M., Bijwe, J. (2009). Influence of orientation of long fibers in carbon fiber-polyetherimide composites on mechanical and tribological properties. *Wear*, 267(5-8): 839-845. <https://doi.org/10.1016/j.wear.2009.01.015>
- [45] AlMuhanna, M., AlMangour, B. (2023). Effect of building orientation and fibre type on the mechanical behaviour of additively manufactured ABS matrix composites. *Materials Research Innovations*, 27(7): 482-489. <https://doi.org/10.1080/14328917.2023.2196480>

- [46] Ramam, R.S., Padal, K.T.B. (2022). Effect of fiber orientation on the mechanical properties of natural fiber epoxy reinforced composites of Flax, Hemp, and Kenaf. *International Journal of Advanced Technology and Engineering Exploration*, 9(86): 72. <https://doi.org/10.19101/ijatee.2021.874747>
- [47] Jesson, D.A., Watts, J.F. (2012). The interface and interphase in polymer matrix composites: Effect on mechanical properties and methods for identification. *Polymer Reviews*, 52(3): 321-354. <https://doi.org/10.1080/15583724.2012.710288>
- [48] Fu, X.L., Li, Y., Schuh, C.A. (2007). Temperature, strain rate and reinforcement volume fraction dependence of plastic deformation in metallic glass matrix composites. *Acta Materialia*, 55(9): 3059-3071. <https://doi.org/10.1016/j.actamat.2007.01.009>
- [49] Laplanche, G., Joulain, A., Bonneville, J., Gauthier-Brunet, V., Dubois, S., El Kabir, T. (2010). Microstructural and mechanical study of an Al matrix composite reinforced by Al-Cu-Fe icosahedral particles. *Journal of Materials Research*, 25(5): 957-965. <https://doi.org/10.1557/JMR.2010.0118>
- [50] Gamstedt, E.K., Skrifvars, M., Jacobsen, T.K., Pyrz, R. (2002). Synthesis of unsaturated polyesters for improved interfacial strength in carbon fibre composites. *Composites Part A: Applied Science and Manufacturing*, 33(9): 1239-1252. [https://doi.org/10.1016/S1359-835X\(02\)00077-5](https://doi.org/10.1016/S1359-835X(02)00077-5)
- [51] Babukiran, B.V., Harish, G. (2014). Influence of resin and thickness of laminate on flexural properties of laminated composites. *International Journal of Engineering Science and Innovative Technology*, 3(1): 279-287.
- [52] Yang, K., Yue, Y.M., Zhao, W.P., Liang, Y., Mei, L., Xue, J.J. (2020). Influence of resin content on mechanical properties of composite laminates. *IOP Conference Series: Materials Science and Engineering*, 770(1): 012009. <https://doi.org/10.1088/1757-899X/770/1/012009>
- [53] El Messiry, M., Eltahan, E., Fathy, S. (2024). Influence of pre-tensioning high-performance yarns on the bending stiffness of textile composites. *Journal of Industrial Textiles*, 54: 15280837241280678. <https://doi.org/10.1177/15280837241280678>
- [54] Brocks, T., Cioffi, M.O.H., Voorwald, H.J.C. (2013). Effect of fiber surface on flexural strength in carbon fabric reinforced epoxy composites. *Applied Surface Science*, 274: 210-216. <https://doi.org/10.1016/j.apsusc.2013.03.018>
- [55] Chabaud, G., Castro, M., Denoual, C., Le Duigou, A. (2019). Hygromechanical properties of 3D printed continuous carbon and glass fibre reinforced polyamide composite for outdoor structural applications. *Additive Manufacturing*, 26: 94-105. <https://doi.org/10.1016/j.addma.2019.01.005>
- [56] Ojha, S., Bisaria, H., Mohanty, S., Kanny, K. (2024). Fractographic analysis of fiber-reinforced polymer laminate composites for marine applications: A comprehensive review. *Polymer Composites*, 45(8): 6771-6787. <https://doi.org/10.1002/pc.28271>
- [57] Oztan, C., Karkkainen, R., Fittipaldi, M., Nygren, G., Roberson, L., Lane, M., Celik, E. (2019). Microstructure and mechanical properties of three dimensional-printed continuous fiber composites. *Journal of Composite Materials*, 53(2): 271-280. <https://doi.org/10.1177/0021998318781938>

NOMENCLATURE

B	Bending modulus, MPa
CF	Carbon fibers
CL	Stainless steel mesh layers
GF	Glass fibers
KF	Kevlar fibers
NR	Natural rubber
UPS	Unsaturated polyester resin
MPa	Megapascals, a unit of pressure or stress